JOURNAL OF MATERIALS SCIENCE 22 (1987) 3276–3286

Shock consolidation of diamond powders

TAMOTSU AKASHI
Center for Explosives Technology Research, New Mexico Institute of Mining and Technology, Socorro, New Mexico 87801, USA

AKIRA B. SAWAOKA
Research Laboratory of Engineering Materials, Tokyo Institute of Technology, Yokohama 227, Japan

Fine and coarse diamond powders were shock-compacted at peak pressures of 77, 90, and 108 GPa. The densification and consolidation mechanisms of diamond powders under shock compression were investigated. The densification behaviour of the diamond powders depended strongly on the particle size of the starting materials. Fine diamond powders were densified primarily by plastic deformation, while coarse diamond powders were densified mainly by particle fracture. The relative densities of the compacted diamond samples increased with an increase in the initial particle size of the diamond and with shock pressure. The consolidation mechanism of the diamond powders under shock compression was closely related to the densification mechanism, and depended on the initial particle size of the diamond. At a shock pressure of 90 GPa, particle sizes of 2 to 4 μm grade and 10 to 20 μm grade were desirable as the starting material in order to produce well-bonded diamond compacts. Diamond compacts having microhardness values over 80 GPa were obtained from 2 to 4 μm grade and 10 to 20 μm grade diamond powders at a shock pressure of 90 GPa, and their relative densities were 88.5% and 91.0%, respectively.

1. Introduction

Carbonardo and ballas are well-known natural polycrystalline diamond masses and have great toughness, superior to that of a single-crystal diamond, and have high hardness. Because of their excellent mechanical properties, these materials have been widely used as cutting tools, drill-bits and wire-drawing dies. The formation processes of carbonardo and ballas are investigated based on observations of their microstructures [1–4]. It is reported that their formation processes are different from each other but that both have an extensive diamond–diamond bonding, leading to high hardness and toughness [2, 3]. However, these natural polycrystalline diamonds are limited in amount, and in wide industrial applications there are some difficulties in shaping and holding these materials. Thus, many efforts for making strong polycrystalline diamond by high-pressure and high-temperature techniques have been made [5, 6].

The sintering of diamond with and without additives at high temperatures and high pressures has been studied [7, 8]. A major difficulty in the sintering of diamond powder without additives is the surface transformation of diamond to graphite during the sintering process [8]. Although sintered diamond compacts with relatively high compressive strengths of 4.5 to 5.8 GPa were produced without additives, the bonding strength between diamond particles in these compacts is considered to be mainly due to the bonding of retransformed graphite [8]. On the other hand, from the studies on additives, it is reported that catalyst metals for diamond synthesis such as cobalt and nickel [9–11] and some appropriate elements such as silicon, boron and beryllium [7] are effective in the sintering of diamond. Among these diamond additive systems, the sintering of diamond with cobalt is considered to be the more attractive and promising method for making strong diamond compacts [12]. Akaishi *et al.* [11] studied the sintering behaviour of diamond in this system (diamond–cobalt) and pointed out that the surface graphitization of diamond particles, which is a harmful phenomenon in the sintering of pure diamond powders, is important for transferring cobalt and, consequently, producing diamond—diamond bonding during the sintering process.

Diamond can be synthesized by shock compression of a low-density phase of carbon as well as by the static high-pressure process [13, 14]. Trueb [15, 16] investigated shock-synthesized diamond powders and found many polycrystalline aggregates, a few tens of micrometres in size, having a substructure very similar to that observed in carbonardo. This suggests that the consolidation of transformed diamond crystallites took place at a high temperature in an extremely short duration of shock pressure, simultaneously with the phase transformation of graphite to diamond.

In the previous papers [17, 18], we reported the dynamic compaction of cubic boron nitride (cBN) powder which is a high-pressure phase of BN. The densification and consolidation processes of cBN powders under shock compression were investigated and well-sintered cBN compacts with 98% theoretical density and a microhardness of 51.3 GPa were obtained from coarse cBN powders (40 to 60 μm grade) [18].

0022–2461/87 $03.00 + .12

The consolidation of diamond crystallites observed in the shock-synthesized diamond powders mentioned above and our previous results on the dynamic compaction of cBN powders, strongly suggest that possibility of consolidation of pure diamond powders into practically large masses by a shock compression technique. In this paper we describe the shock consolidation of diamond powders.

2. Experimental procedure

2.1. Starting materials

Commercial-grade, synthetic diamond powders with different grain sizes were used as the starting materials. These powders were provided by General Electric Co. Ltd and were of 0 to 1/2, 2 to 4, 10 to 20 and 40 to 60 μm grades. Scanning electron micrographs of the as-received diamond powders are shown in Fig. 1. Particle morphology, especially in the coarse grade powders, suggests that these diamond powders were seived and refined through a crushing operation after synthesis. A spectrochemical analysis of the impurities in the 2 to 4 μm grade and 40 to 60 μm grade powders is listed in Table I. The powders without additives were pressed into stainless steel capsules [19] to form discs 5 mm thick and 12mm diameter with a density of 60% theoretical density. Then they were explosively shock-compacted.

TABLE I Spectrochemical analysis of starting diamond powders

2 to 4 μm grade powder		40 to 60 μm grade powder	
Element	Wt (p.p.m.)	Element	Wt (p.p.m.)
Si	800	Si	800
Mg	10	Mn	10
Ni, Cu, Ca	5	Ni, Cu, Ca	5
Al, Cr	1	Fe, Mg, Al	1

2.2. Shock-compaction experiments

Shock treatments were carried out using a mouse-trap type plane wave generator and a momentum trap recovery system. Details of the shock-treatment fixture have been reported elsewhere [19]. The iron flyer plane used was 4.3 mm thick and the impact velocities employed in this experiment were 2.1, 2.5 and 3.0 km sec^{-1}. The shock pressures induced in the

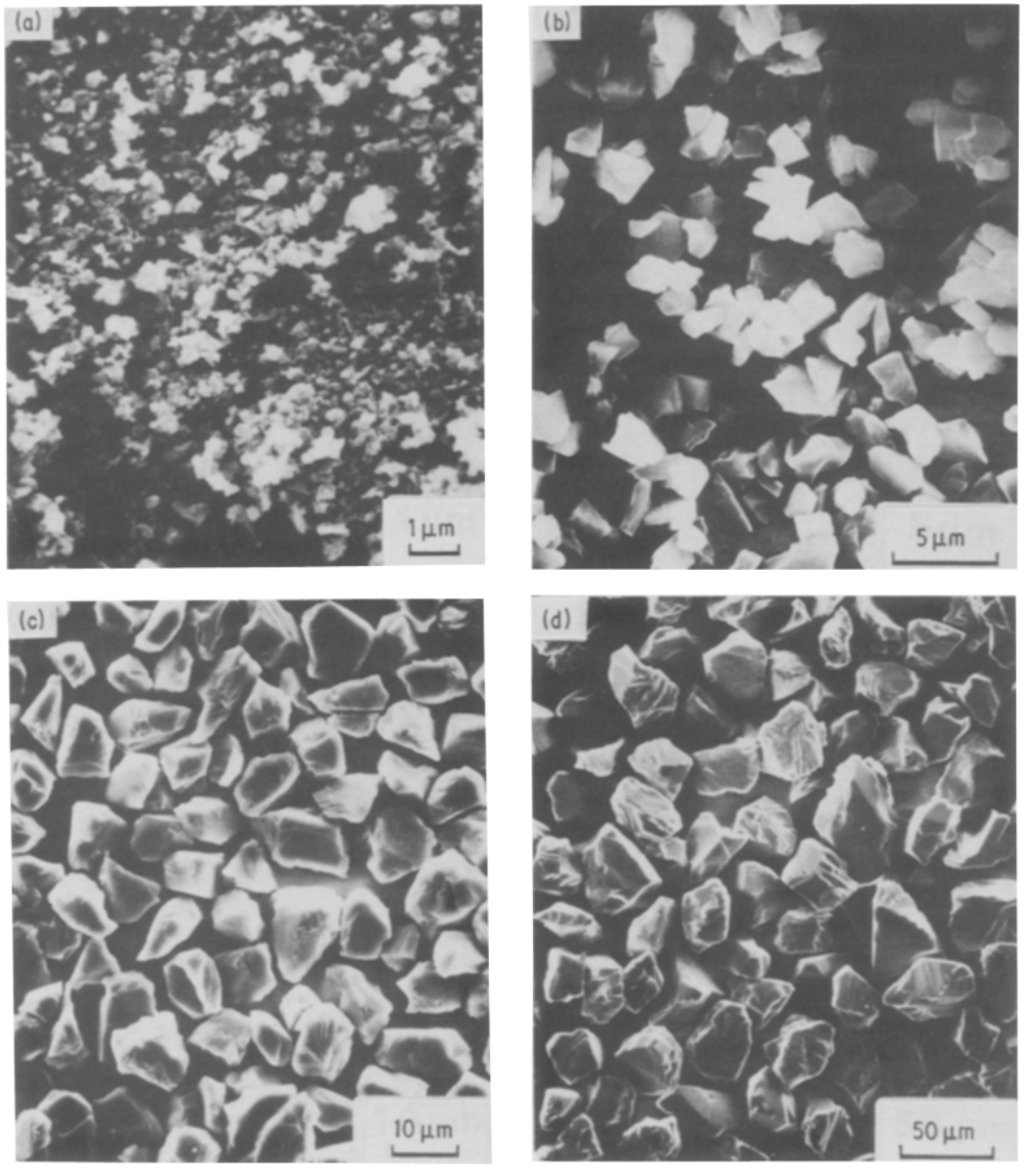

Figure 1 Scanning electron micrographs of starting diamond powders. (a) 0 to 1/2 μm, (b) 2 to 4 μm, (c) 10 to 20 μm and (d) 40 to 60 μm grade diamond powders.

diamond powder compacts at these impact velocities were not calculated, but a calculation for titanium dioxide (rutile-type) powder has been performed using the two-dimensional CSQ computer code at an impact velocity of 2.5 km sec^{-1} [20]. Thus, approximate peak pressures in the powder compacts at 2.1 and 3.0 km sec^{-1} were obtained by scaling the pressures in [20]. Peak pressures at the outer and centre regions within the powder compacts differ significantly and are estimated to be 33 and 77 GPa, 40 and 90 GPa and 48 and 108 GPa for the outer and centre regions at impact velocities of 2.1, 2.5 and 3.0 km sec^{-1}, respectively. Immediately after impact, fixtures containing the capsules were plunged into a water basin and quickly cooled before being recovered. After the shock treatments, compacted samples were carefully taken out of the capsules using a lathe.

2.3. Characterization of compacted diamond powders

In the shock-treatment fixture employed in this work, the shock pressure depends strongly on the radial position within the powder compacts mentioned above, while the shock temperature differs remarkably in the top and bottom regions at a given impact velocity [20]. The positions correspond to the direction of impact of the flyer plate to the capsules. In our previous studies [18, 19, 21] on shock consolidation of some ceramic powders using a shock-treatment fixture identical to the fixture used in this work, the distribution and history of the shock temperature within the powder compacts rather than those of shock pressure, had a significant effect on their consolidations. Because of this, in this work the resultant diamond compacts were characterized with respect to the top and bottom regions by means of X-ray diffraction, Vicker's microhardness test and scanning electron and optical microscopy.

Both surfaces of each diamond compact recovered were ground using a diamond wheel and then polished with 10 to 20 and 0 to 1 μm diamond powders. After polishing, densities of the diamond compacts were measured by the water displacement method. Vicker's microhardness values were measured on the polished surfaces of the compacts using 4.9 and 9.8 N loads with a loading time of 15 sec. The phases present in the recovered compacts were examined using an X-ray diffractometer with nickel-filtered CuKα radiation. The residual lattice strain and the crystallite size of the compacted diamond powders were determined by X-ray line-broadening analysis using the Hall equation [22] referring to well-annealed alumina powder. X-ray diffraction patterns of the samples for the phase identification and the line-broadening analysis were also taken on the polished top and bottom surfaces of the compacts. Microstructures of the fracture and polished surfaces of the compacted diamond samples were examined by scanning electron (SEM) and optical microscopy.

3. Results and discussion

3.1. Appearance of recovered diamond compacts

Compacted diamond samples were recovered as a whole disc containing many cracks, except for the samples produced at 108 GPa which were broken into few pieces at recovery. Fig. 2 shows the polished top and bottom surfaces of the diamond compacts obtained from the (a) 0 to 1/2 μm, (b) 2 to 4 μm, (c) 10 to 20 μm and (d) 40 to 60 μm grade powders at 90 GPa. Bright regions, most noticeably in the compacted fine powders, correspond to the regions where diamond particles or agglomerates were taken out during the grinding and polishing operations. The number of cracks generated in the compacted diamond powders tends to increase with an increase in the particle size of the starting diamond powders, as seen in Fig. 2. This is the same tendency as was observed in the dynamic compaction of cBN powders [17, 18]. Furthermore, in each compact there were fewer cracks in the top surface than in the bottom surface. This seems to be related to a difference in microhardness in the surfaces. Also, the cracking behaviour observed in Fig. 2 is related to the rarefaction wave associated with the intense radial shock wave generating from the outer part of the bottom region as predicted by the two-dimensional simulation [20].

The diamond compacts obtained at 77 GPa had fewer cracks, independent of the initial diamond particle size, than those produced at 90 and 108 GPa, but the microhardness values of the compacts were considerably low, near 10 GPa.

3.2. Microhardness and density of diamond compacts

Fig. 3 shows the dependence of the relative density of the compacted diamond powders on the initial particle size of the diamond. In this figure, 0 to 1/2, 2 to 4, 10 to 20 and 40 to 60 μm grade powders are represented by their mean particle sizes of 1/4, 3, 15 and 50 μm, respectively. Density of the 2 to 4 μm grade powder compacted at 108 GPa could not be measured because the compacts were broken into small pieces. The relative densities of the diamond compacts produced at 77 and 90 GPa increased gradually with an increase in the initial particle size and with shock pressure. The dependence of the relative density on the initial particle size qualitatively agrees with that observed in the dynamic compaction of cBN powders [18], but the relative densities reached at 77 GPa differ significantly between the diamond and cBN powders. The relative density of the compacted 40 to 60 μm grade cBN powder was 98%, while the 40 to 60 μm grade diamond powder showed no greater than 89% theoretical density. Although it is necessary to consider an effect of a large number of cracks in the recovered diamond compacts on the density, the lower relative density of the compacted diamond powders indicates that densification of diamond powder under shock compression is much harder than that of cBN powder. This may be caused by the excellent mechanical properties of diamond at high temperatures [23, 24].

The dependence of the microhardness of the compacted diamond samples on the particle size of the starting diamond powders is shown in Fig. 4. Also, the dependence of the microhardness on shock pressure is shown in Figs 5 and 6. At 77 GPa the microhardness

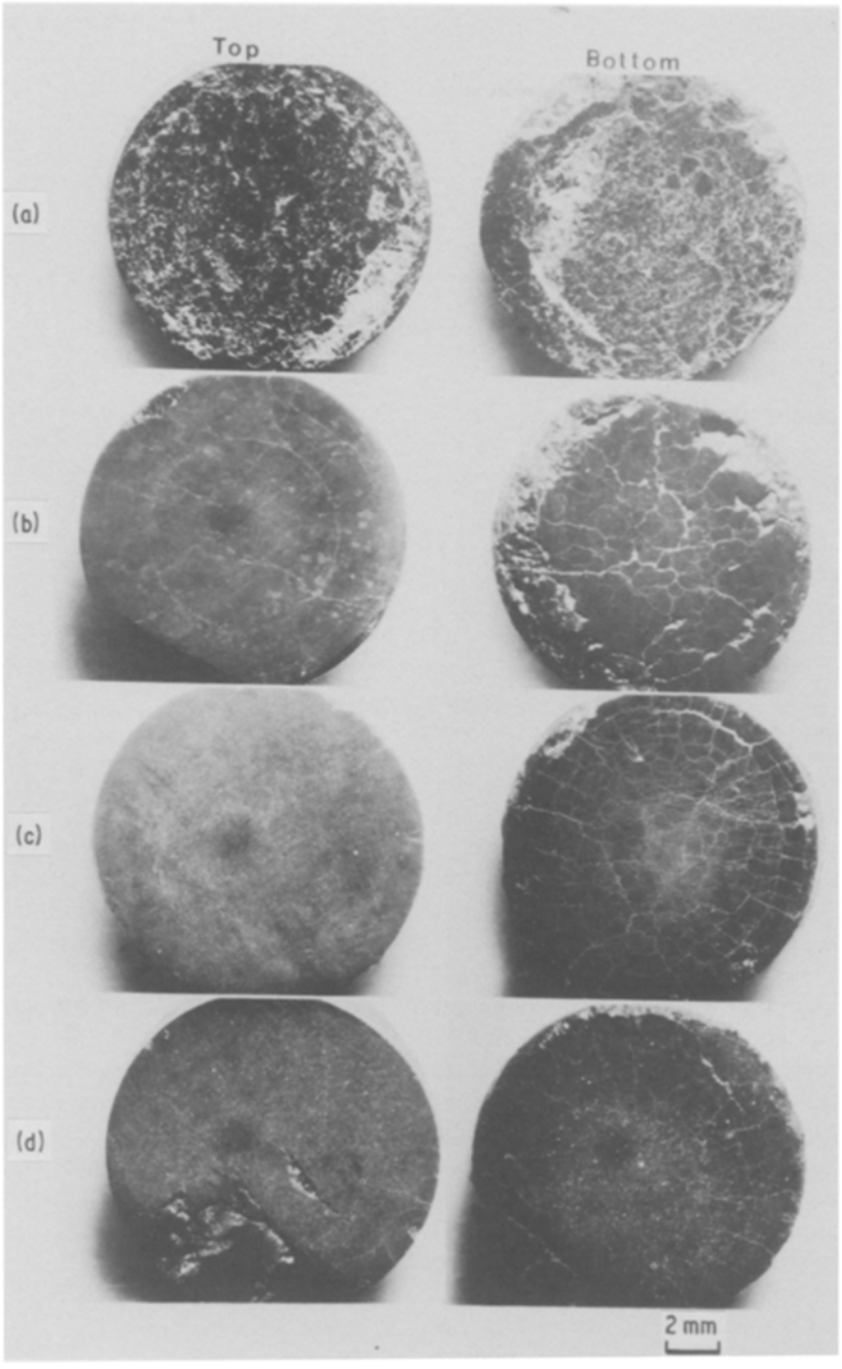

Figure 2 Sectional views of polished top and bottom surfaces of (a) 0 to 1/2 μm, (b) 2 to 4 μm, (c) 10 to 20 μm and (d) 40 to 60 μm powders compacted at 90 GPa.

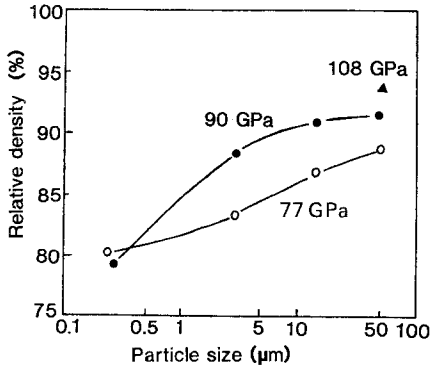

Figure 3 Dependence of relative density of compacted diamond powders on initial particle size of diamond.

values of the diamond compacts were very low, near 10 GPa, and little dependence on the initial particle size was shown. As shock pressure increased from 77 to 90 GPa, microhardness values increased significantly, especially in the bottom surfaces of the compacts, and clearly showed large dependence on the initial diamond particle size. A maximum microhardness value of 84 GPa was obtained in the bottom surface of the 2 to 4 μm grade powder compacted at 90 GPa, which is equivalent to microhardness values reported in the static high-pressure sintering of pure diamond powders [7]. The compacted 10 to 20 μm grade powder (at 90 GPa) also had microhardness of 82 GPa. At a shock pressure of 90 GPa, as the initial particle size decreased to smaller than 2 to 4 μm grade or increased

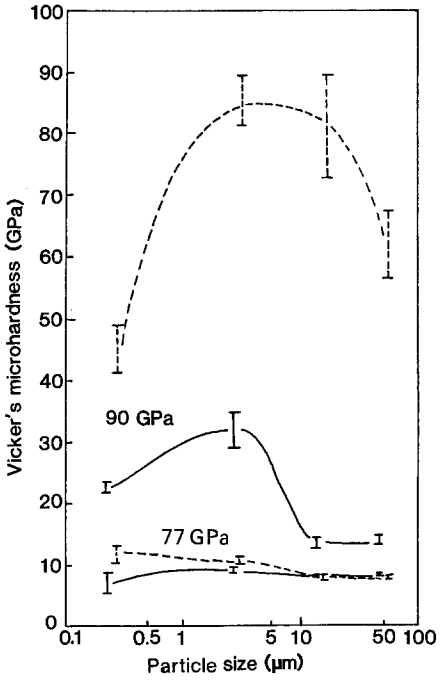

Figure 4 Dependence of microhardness of compacted diamond powders on initial particle size of diamond.

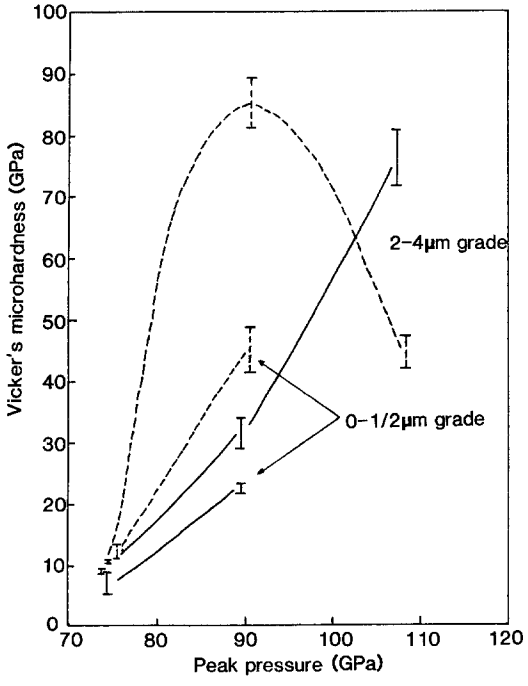

Figure 5 Dependence of microhardness of compacted diamond powders on shock pressure. Initial particle sizes of diamond are 0 to 1/2 and 2 to 4 μm grade. (——) Top surface, (– – –) bottom surface.

to larger 10 to 20 μm grade, microhardness of the compacted diamond samples tended to decrease as seen in Fig. 4. The dependence of microhardness on the initial particle size, which is different from that observed in the dynamic compaction of cBN powders [18], seems to be closely related to both the densification and consolidation mechanisms of diamond powders under shock compression.

The large difference in the microhardness values between the top and bottom surfaces of each diamond compact obtained at 90 GPa is apparently due to the difference in the temperature history in both the regions during shock compression. This is a more distinguishable phenomenon than in the compacted cBN powders [18], and suggests that the densification and consolidation of diamond powders under shock compression of 90 GPa were more sensitive to the temperature and its history within the powder compact than to shock pressure. On the other hand, with an increase in shock pressure from 90 to 108 GPa, the microhardness values in the top and bottom surfaces of the compacted samples tended to be close to each other as seen in the results of the compacted 2 to 4 and 40 to 60 μm grade powders (Figs 5 and 6). The microhardness of the top surface of the compacted 2 to 4 μm grade powder increased remarkably with the increase in shock pressure, but in the bottom surface the microhardness value was reduced significantly by the conversion of the diamond to graphite (Fig. 7c). In the bottom surface of the compacted 40 to 60 μm grade powder, a small amount of graphitization of diamond was detected. Because of this, the microhardness of this surface increased little with the increase in shock pressure. Thus, a diamond compact having nearly equal microhardness in both the top and bottom surfaces can be produced from 2 to 4 μm grade powder at about 102 GPa and from 40 to 60 μm grade powder at about 112 GPa according to Figs 5 and 6. In these cases, microhardness of the diamond compacts is expected to be about 60 GPa, but a small amount of graphitization of the diamond may occur in the bottom surfaces of the compacts.

3.3. Densification mechanism of diamond powders

Densification of powder compacts in the dynamic-compaction process is thought to occur mostly at the shock wave front. Ceramic powders can be densified mainly by means of particle fracture and/or plastic deformation of particles under shock compression.

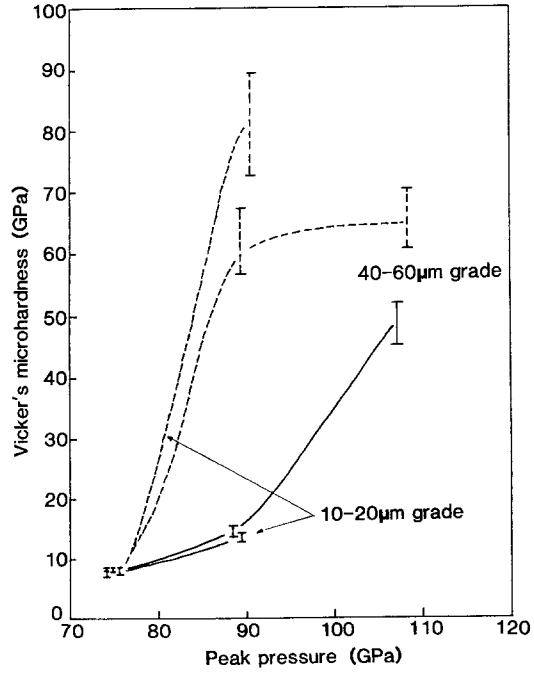

Figure 6 Dependence of microhardness of compacted diamond powders on shock pressure. Initial particle sizes of diamond are 10 to 20 and 40 to 60 μm grade. (——) Top surface, (– – –) bottom surface.

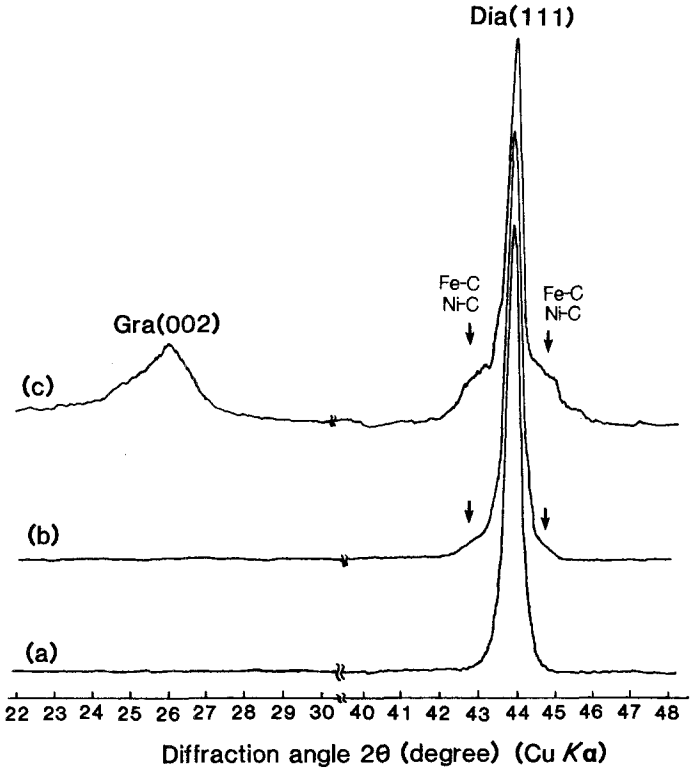

Figure 7 X-ray diffraction patterns of compacted 2 to 4 μm grade powders. Patterns (a), (b) and (c) are taken using the bottom surfaces of compacts obtained at 77, 90 and 108 GPa, respectively.

The former densification mechanism, particle fracture, usually results in a large particle size reduction in compacted powders, and the latter mechanism, plastic deformation, brings about a significant increase in lattice strain in the recovered materials [19]. Figs 8 and 9 show the residual lattice strain and crystallite size in the diamond powders compacted at 77, 90 and 108 GPa. At 77 GPa, the lattice strain values in the recovered diamond compacts were less than 0.05% and showed no appreciable dependence on the initial particle size of the diamond. Such small lattice strain in the compacts suggests that diamond powders were densified by particle fracture under shock compression of 77 GPa. However, the SEM observations of fracture surfaces of the compacts obtained at 77 GPa indicated that there was no significant particle size reduction in the compacted 0 to 1/2 and 2 to 4 μm grade powders, while in the compacted 10 to 20 and 40 to 60 μm grade powders, the particle size was reduced remarkably by the shock compression. Therefore, it is concluded that it is possible to densify the 0 to 1/2 and 2 to 4 μm grade powders by plastic deformation of particles but that shock pressure and temperature were, in fact, not sufficiently high to create plastic deformation in these powder compacts, resulting in little change in lattice strain and particle size. On the other hand, the 10 to 20 and 40 to 60 μm grade powders appear to be densified mainly by particle fracture under shock compression. With an increase in shock pressure from 77 to 90 GPa, the increase in lattice strain in the recovered diamond compacts depended on the initial particle size of the diamond. In the compacted 2 to 4 μm grade powder, the lattice strain increased significantly to 0.23% and 0.18% for the top and bottom surfaces, respectively, while in the compacted 0 to 1/2 μm grade powder, the increase in the lattice strain was appreciable (Fig. 8). As the particle size increased from 2 to 4 to 10 to 20 and 40

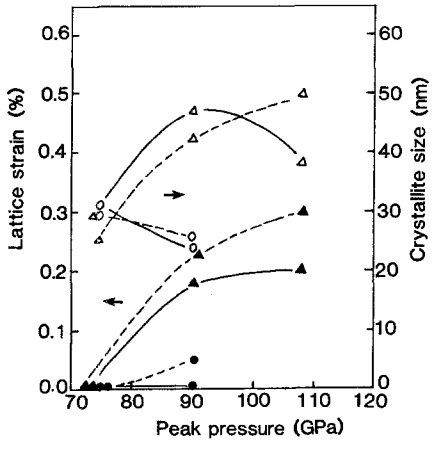

Figure 8 Residual lattice strain and crystallite size in compacted (○, ●) 0 to 1/2 and (△, ▲) 2 to 4 μm grade powders. (——) Top surface, (– – –) bottom surface.

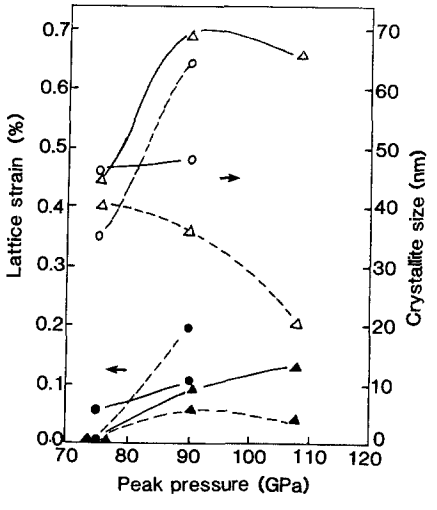

Figure 9 Residual lattice strain and crystallite size in compacted (○, ●) 10 to 20 and (△, ▲) 40 to 60 μm grade powders. (——) Top surface, (– – –) bottom surface.

to 60 μm grade, the lattice strain gradually decreased. Figs 10 and 11 show optical micrographs of the polished bottom surfaces and scanning electron micrographs of fracture surfaces in the bottom regions of the diamond compacts obtained at 90 GPa. These photographs clearly show changes in the size and the shape of the diamond particles due to shock treatments. There was no appreciable change in the particle size of the diamond in the compacted 0 to 1/2 and 2 to 4 μm grade powders, but there was remarkable change in the compacted 10 to 20 and 40 to 60 μm grade powders relative to the initial particle size. This is the same phenomenon as was observed in the compacts obtained at 77 GPa. Fig. 12 shows a low-magnification photograph of the polished bottom surface of the compacted 40 to 60 μm grade powder (at 90 GPa), corresponding to Fig. 10d. From the comparisons of this figure and Figs 10c, and 11c and d, the particle size reduction of the diamond in the compacted 40 to 60 μm grade powder was remarkable in comparison with that in the compacted 10–20 μm grade powder. From the residual lattice strain and particle size reduction found in the recovered diamond compacts, it is concluded that the 0 to 1/2 and 2 to 4 μm grade fine diamond powders were densified primarily by plastic deformation of particles under shock compression of 90 GPa, while the 40 to 60 μm grade coarse powder was densified mainly by particle fracture. The 10 to 20 μm grade powder can be densified by both the mechanism of particle fracture and that of plastic deformation. Also, at 108 GPa, fine and coarse diamond powders were densified by plastic deformation and particle fracture, respectively. Therefore, the dependence of densification behaviour of diamond powders on the initial particle size of diamond is unchanged in the shock pressure range from 77 to 108 GPa employed in this experiment.

The amount of plastic deformation during the densification process in the compacted 0 to 1/2 μm grade powder, estimated from the residual lattice strain in the recovered compact, was appreciable even at 90 GPa. This can be explained by the following two factors. One is the effective stress being applied to each particle under shock compression, which decreases with a decrease in particle size. Another is the strength of the particle, which generally increases with a decrease in particle size [25]. Stupkina [26] has investigated dependence of the impact strength of a diamond on particle size and reported that the strength of diamond particles was inversely proportional to the diamond particle size. Thus, in dynamic compaction of 0 to 1/2 μm grade powder, local stress applied to each diamond particle at a shock pressure of 90 GPa seems to be lower than that in the compacted 2 to 4 μm grade powder. Furthermore, each particle of 0 to 1/2 μm grade powder seems to have greater strength than that of each particle of the 2 to 4 μm grade powder. Therefore, the plastic deformation in the compacted 0 to 1/2 μm grade powder during shock compression became considerably less than that in the compacted 2 to 4 μm grade powder, even when shock pressure and temperature conditions were the same.

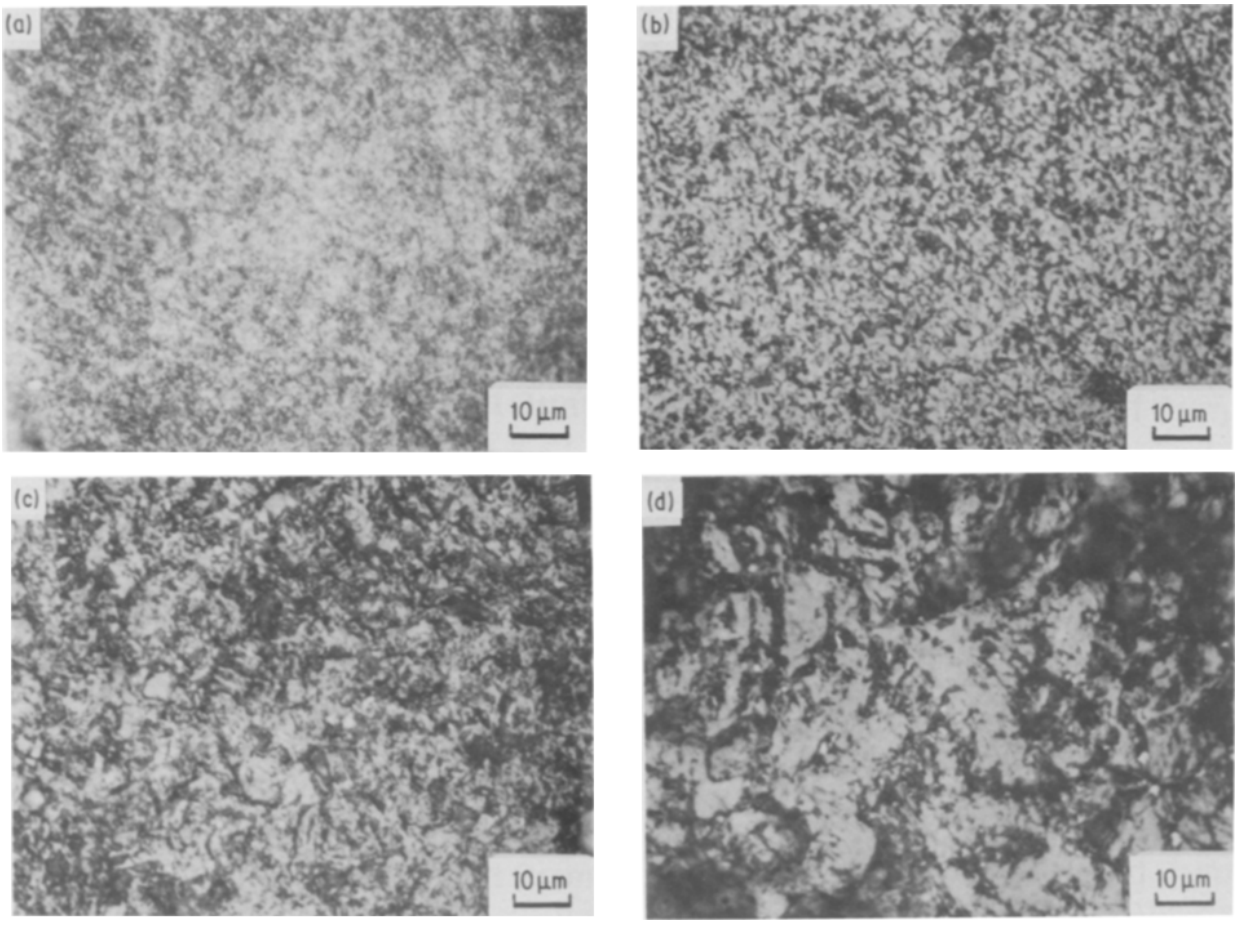

Figure 10 Optical micrographs of polished bottom surfaces of compacted (a) 0 to 1/2 μm, (b) 2 to 4 μm, (c) 10 to 20 μm and (d) 40 to 60 μm grade powders (at 90 GPa).

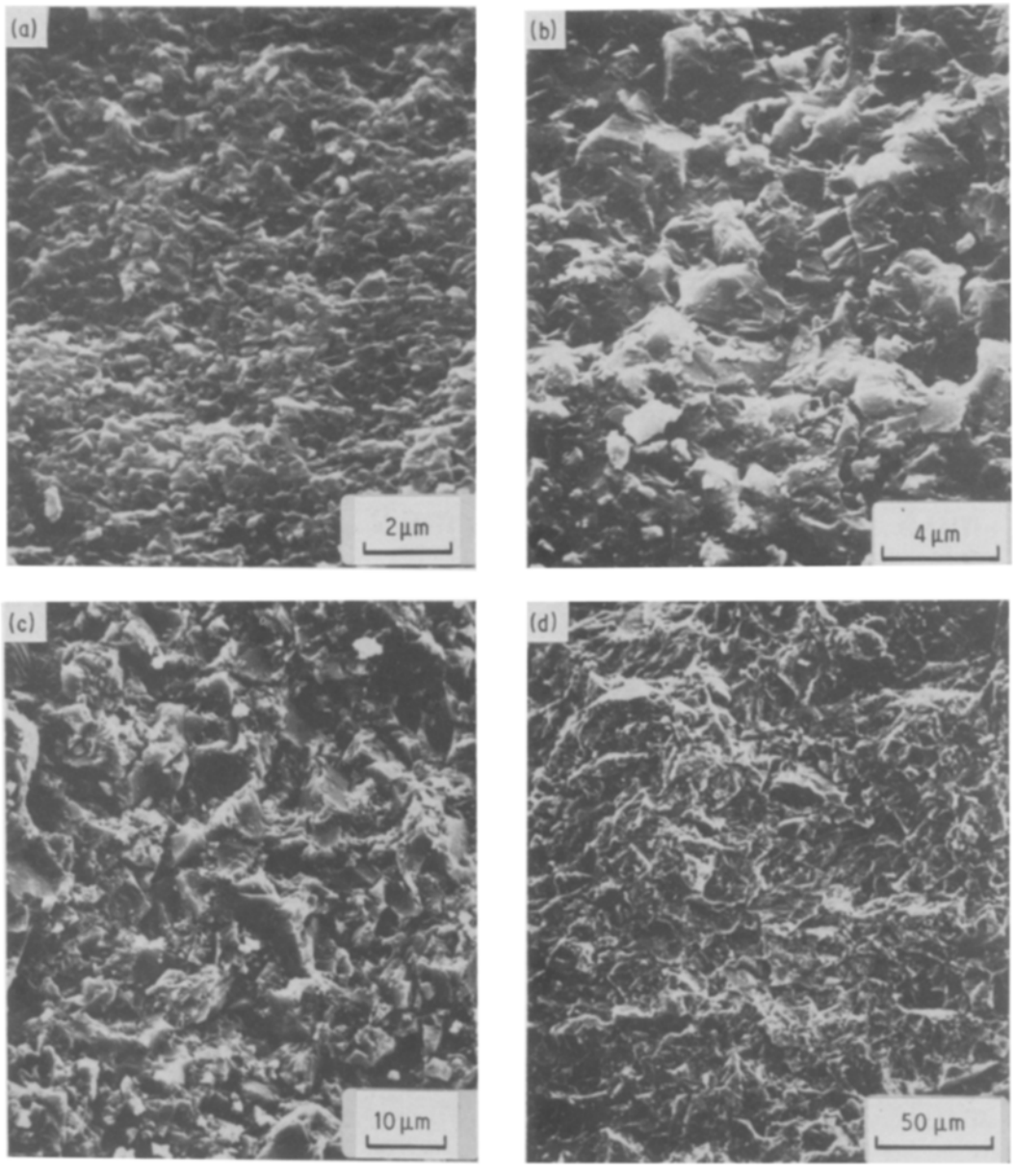

Figure 11 Scanning electron micrographs of fracture surfaces near the centre parts of the bottom surfaces of compacted (a) 0 to 1/2 μm, (b) 2 to 4 μm, (c) 10 to 20 μm and (d) 40 to 60 μm grade powders (at 90 GPa).

Such powder compaction behaviour in the 0 to 1/2 μm grade powder under shock compression is primarily responsible for the low relative density and low microhardness of its resultant compacts. High microhardness values of the compacted 2 to 4 μm grade and 10 to 20 μm grade powders indicate that at a shock pressure of 90 GPa, particle sizes of 2 to 20 μm are most suitable for making strong diamond compacts by dynamic compaction. On the other hand, the compacted 40 to 60 μm grade powder revealed a small amount of lattice strain, showing a little plastic deformation during the dynamic-compaction process, even though the coarse diamond powder is densified mainly by particle fracture by the shock treatment mentioned before. This implies that small fragments of a few micrometres in size, produced from coarse particles through particle fracture by a passage of the shock front, deformed plastically during shock compression and brought about additional densification of the compact. The fracture features of a diamond particle when loaded indicate that the densification speed of the coarse diamond powder (40 to 60 μm grade) under shock compression by means of particle fracture might be very fast. The crack velocity in diamond crystal is reported to be more than 7.5 km sec^{-1} [27], which is lower than the shock wave velocity in diamond being shock compressed at 90 GPa, but about three times higher than the particle velocity [28]. This strongly suggests that the coarse diamond powder can be densified very rapidly by particle fracture at the shock wave front into high density, and then resultant small fragments of diamond deformed plastically during shock compression, resulting in the additional densification of the powder.

The crystallite size of the diamond in the recovered compacts also varied with the initial particle size of the diamond and with shock pressure. Except for the compacted 40 to 60 μm grade powder, the variation of the crystallite size with shock pressure almost corresponds to the variation of the residual lattice strain and microhardness with shock pressure as seen in Figs 5 to 7 and 9. The increase in the crystallite size with shock pressure, observed in the compacted 2 to 4 and 10 to 20 μm grade powders, is a unique feature in the

dynamic compaction of diamond powders. This may imply that the growth of crystallites produced during the densification took place simultaneously with the consolidation. The uniqueness of the crystallite size change in the compacted 40 to 60 μm grade powder may be related to the densification mechanism of this powder under shock compression and to the pressure distribution and history within the powder compact during the dynamic-compaction process.

Thus, it is concluded that the densification mechanism of diamond powders under shock compression strongly depends on the initial particle size of the diamond powders, but does not depend on shock pressure in the pressure range from 77 to 108 GPa. The relative densities of the compacted diamond samples increased with the increase in the initial diamond particle size and reached 93% in the 40 to 60 μm grade powder compacted at 108 GPa. The variation in the microhardness values of the resultant compacts (at 90 and 108 GPa) is not related to the relative density but is closely related to the densification mechanism depending on the initial particle size of the diamond.

3.4. Consolidation mechanism of diamond powders

The densification mechanism of a powder compact under shock compression is closely related to the degree of interparticle bonding developed during the dynamic-compaction process, because the localized high temperature rise is associated with the powder densification and plays an important role in producing that bonding [29–31]. Specifically, the high temperature rise at the grain boundaries resulting from intense plastic deformation in the contact surfaces of particles during the densification is significant in the shock consolidation of powders [19]. Furthermore, our previous work [18] on the dynamic compaction of cBN powders showed the strong effects of particle size of the starting materials on the consolidation of the powders. That consolidation of cBN powders was enhanced with an increase in the initial particle size reflected the fact that localized temperature in the compacted coarse cBN powder was higher than in the compacted fine powder.

In the dynamic compaction of diamond powders, the densification mechanism depended strongly on the initial particle size of the starting materials as mentioned before. The 40 to 60 μm grade coarse powder was densified mainly by particle fracture in the shock pressure range of 77 to 108 GPa. Therefore, little temperature rise at the contact surfaces of particles caused by plastic deformation during the densification may occur in this compact, though the heating resulting from frictional rubbing and the shock compression of gases in the pores can still be expected. Such localized heating can occur at particle boundaries that are in the initial powder compact, but that are not related to grain boundaries newly induced within the coarse diamond particles by fracturing during the densification. This may be the reason why the consolidation of the fine grains produced by fracturing coarse particles took place locally, as seen in Fig. 12. This is also why the microhardness value of the compacted 40 to 60 μm grade powder is lower than the microhardness values of the compacted 2 to 4 and 10 to 20 μm grade powders. On the other hand, the 2 to 4 μm grade diamond powder was densified by plastic deformation of particles in the pressure range from 77 to 108 GPa. Thus, in this powder compacted at 90 GPa, judging from the high residual lattice strain in the recovered sample, intense plastic deformation may have resulted in a localized high temperature rise at the grain boundaries producing interparticle bonding in the compact during shock compression. In the 0 to 1/2 μm grade diamond powder, even at 90 GPa, plastic deformation of particles was very limited because of the low effective stress in each particle and the high strength of fine diamond particles. This caused the low relative density and low microhardness of the compacted 0 to 1/2 μm grade powder. In dynamic compaction of the 10 to 20 μm grade powder, consideration of the densification mechanism shows that the powder can be consolidated by both the mechanisms proposed above.

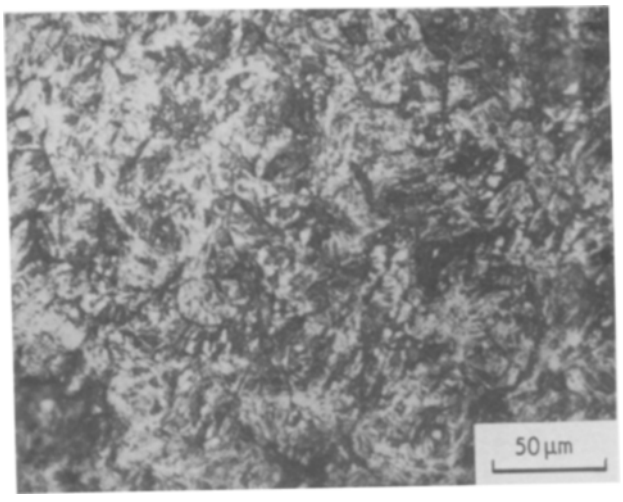

Figure 12 Microstructure of polished bottom surface of compacted 40 to 60 μm grade powder (at 90 GPa).

In Fig. 10, bright regions correspond to well-consolidated regions with strong interparticle bonding. As the initial particle size increased, such consolidated regions observed in these polished surfaces decreased gradually and the distribution of such regions became non-uniform as seen in the photographs. The relatively large bright regions seen in Figs 10c and d were found to consist of particles of few micrometres which were bonded each other. The microstructures in Figs 10b and c correspond to the regions where the microhardness values were 84 and 82 GPa, respectively. The amount of interparticle bonding observed in the photographs was, in fact, less than that supposed from such high microhardness values. This contradiction can be explained partly by the extremely strong diamond–diamond bonding and partly by the small particle size of the diamond after shock compression compared to the size of the indentation of 14 to 16 μm in microhardness measurements. The strong direct bonding seems to result in high microhardness, even though the apparent amount of interparticle bonding was small. Also, the small particle size of the diamond can increase microhardness because the indentation is covered by many fine

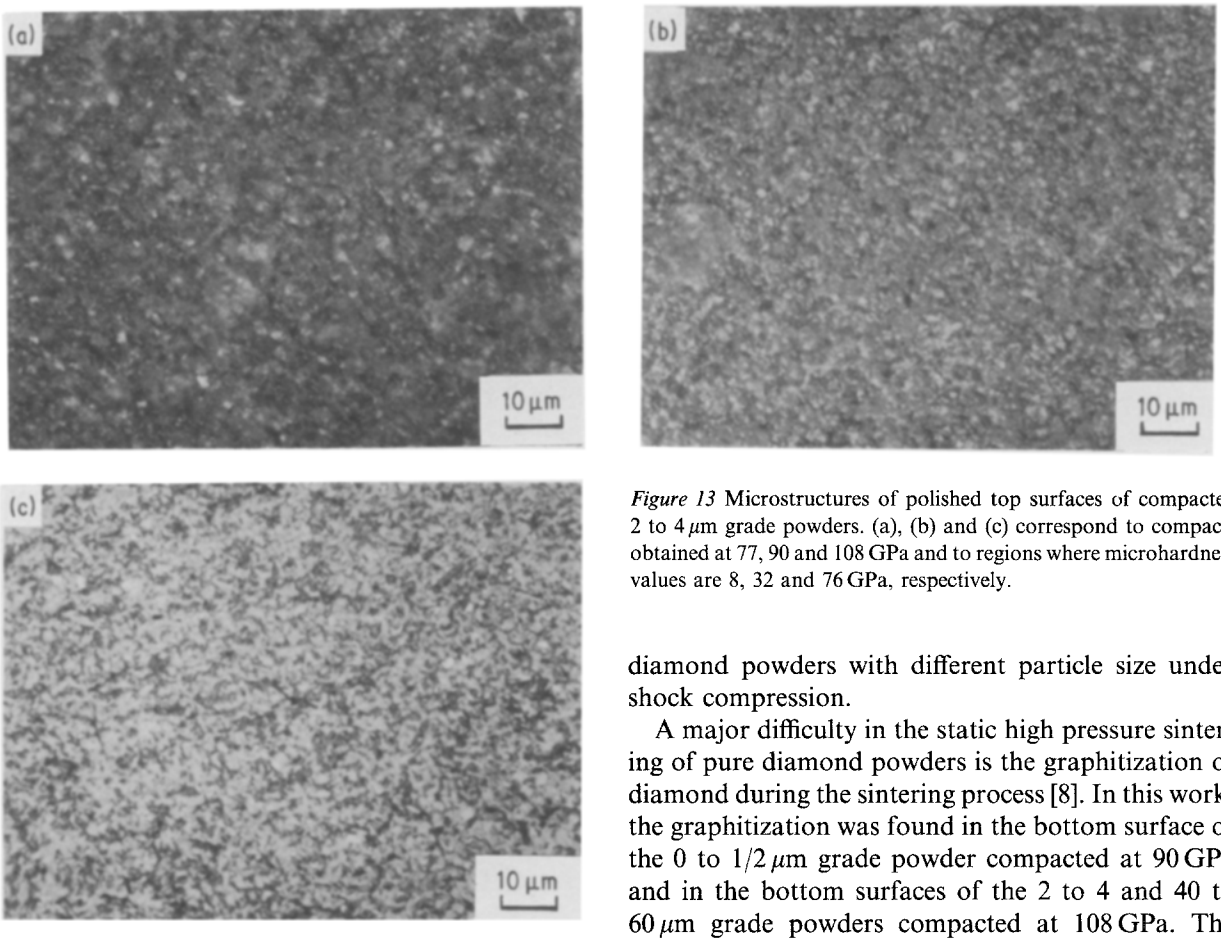

Figure 13 Microstructures of polished top surfaces of compacted 2 to 4 μm grade powders. (a), (b) and (c) correspond to compacts obtained at 77, 90 and 108 GPa and to regions where microhardness values are 8, 32 and 76 GPa, respectively.

particles and its extension can be constrained by the grain boundaries.

The microstructures in the polished top surfaces of the compacted 2 to 4 μm grade powders (at 77, 90 and 108 GPa) are shown in Fig. 13. In this figure, (a), (b) and (c) correspond to the regions where microhardness values were 8, 32 and 76 GPa, respectively. The increase with shock pressure in bright regions in these microstructures is very consistent with the increase in the microhardness, indicating the increase in the formation of interparticle bonding. This implies that the formation of interparticle bonding in diamond powder compacts can be remarkably increased by increasing the shock temperature, because increasing shock pressure corresponds increasing shock temperature in the shock compaction of powder compacts with an equal initial density [32].

In the observations of fracture surfaces of the compacted diamond samples, intergranular fracture was found locally in the bottom regions of the 2 to 4 μm grade powder compacted at 90 GPa. Such regions may correspond to the regions where interparticle bonding was observed in the polished surface (Fig. 10b). This is evidence of strong interparticle bonding locally developed in this compact. The observations of the polished and fracture surfaces of the compacted diamond samples mentioned above are very consistent with the results of microhardness measurements. In addition, the variation in the microstructures of the resultant diamond compacts with the initial particle size of the diamond agrees well with the variations in the densification and consolidation mechanisms of diamond powders with different particle size under shock compression.

A major difficulty in the static high pressure sintering of pure diamond powders is the graphitization of diamond during the sintering process [8]. In this work, the graphitization was found in the bottom surface of the 0 to 1/2 μm grade powder compacted at 90 GPa and in the bottom surfaces of the 2 to 4 and 40 to 60 μm grade powders compacted at 108 GPa. The amount of graphite formation in the bottom surface of the compacted 2 to 4 μm grade powder (108 GPa) was estimated from X-ray diffraction analysis (Fig. 7c) to be about 10%. This is primarily responsible for the rapid reduction of the microhardness in the bottom surface of this compact with the increase in shock pressure from 90 to 108 GPa. However, it is surprising that the bottom surface of this compact still exhibited a high microhardness of 44 GPa (Fig. 5). In the other two compacts, the graphitization of diamond was a trace, and the effect of the graphitization on the microhardness seems to be insignificant considering the result mentioned above. The recovered diamond compacts had relatively low relative densities. This suggests a possibility of the graphitization of the diamond during the shock compression as well as after the release of the shock pressure.

Fig. 7 shows X-ray diffraction patterns taken of the polished bottom surfaces of the diamond compacts produced from the 2 to 4 μm grade diamond powders at (a) 77, (b) 90 and (c) 108 GPa. Weak diffraction lines on both sides of the (1 1 1) diffraction line for diamond were detected in (b) and (c). Electron probe X-ray micro-analysis (EPMA) showed that the main impurities in these two samples were iron and nickel from the stainless steel capsule. These impurities were found to be concentrated in the crack regions observed in the recovered compacts (Fig. 2). Therefore, from the impurity analysis, the weak diffraction lines mentioned above can be identified with the lines for Fe–C and Ni–C compounds which were produced during or after shock compression. The effect of these impurities on the consolidation of diamond powders is not clear, but the following comparison of microhardness

suggests that this effect is not significant. The amount of the impurities, estimated from X-ray diffraction analysis, in the two top surfaces of the 2 to 4 μm grade powders compacted at 90 and 108 GPa were almost equal, but their microhardness values differed significantly. The former had 32 GPa, while the latter had 76 GPa. It is clear that this increase in microhardness was caused by an increase in shock pressure and temperature, but that it is not related to the amount of the impurities in these compacts.

Thus, it is concluded that the consolidation mechanism of diamond powders under shock compression is closely related to the densification mechanism of the powders, and depends strongly on the initial particle size of the diamond. Plastic deformation of particles during the densification process has an important role in the shock consolidation of diamond powders. In order to produce well-bonded diamond compacts by dynamic compaction at a shock pressure of 90 GPa, diamond powders with particle sizes of 2 to 20 μm are desirable as the starting material.

4. Conclusions

Fine and coarse diamond powders were shock-compacted at peak pressures of 77, 90 and 108 GPa and the densification and consolidation mechanisms of diamond powders under shock compression were studied. The densification behaviour of diamond powders depended strongly on the particle size of the starting diamond powders. The 0 to 1/2 and 2 to 4 μm grade fine diamond powders were densified primarily by plastic deformation, while 40 to 60 μm grade coarse powder was densified mainly by particle fracture. The 10 to 20 μm grade powder was densified by both mechanisms. The relative densities of the compacted diamond samples increased with an increase in the initial particle size of the diamond and with shock pressure.

The consolidation behaviour of the diamond powders under shock compression was closely related to the densification mechanism of the powders and also depended on the initial particle size of the diamond. The results of microhardness measurements indicate that the optimum shock compaction condition for producing strong diamond compacts depends on the particle size of the starting diamond powder. At a shock pressure of 90 GPa, particle sizes of 2 to 4 and 10 to 20 μm grade were suitable. The large difference in the microhardness in the top and bottom surfaces of each compact (at 90 GPa) suggests that the consolidation of diamond powders by shock compression is more sensitive to shock temperature than to shock pressure, and that high temperatures are required for the consolidation of diamond powders, i.e. higher temperatures than those required for the consolidation of cBN powders. Diamond compacts having microhardness values over 80 GPa were produced from the 2 to 4 and 10 to 20 μm grade powders at a shock pressure of 90 GPa. Their relative densities were 88.5% and 91.0%, respectively.

Acknowledgement

This work was performed with funding from the state of New Mexico Economic Development and Tourism Department through the Center for Explosives Technology Research of New Mexico Institute of Mining and Technology.

References

1. I. V. NIKOL'SKAYA, L. F. VERESHCHAGIN, YU. L. ORLOV, E. M. FEKLICHEV, and YA. A. KALASHNIKOV, *Sov. Phys. Dok.* **13** (1969) 881.
2. L. F. TRUEB and W. C. BUTTERMAN, *Am. Mineral.* **54** (1969) 3.
3. L. F. TRUEB and C. S. BARRETT, *ibid.* **57** (1972) 1664.
4. Y. MORIYOSHI, M. KAMO, N. SETAKA and Y. SATO, *J. Mater. Sci.* **18** (1983) 217.
5. YA. A. KALASHNIKOV, L. F. VERESHCHAGIN, E. M. FEKLICHEV and I. S. SUKHUSHINA, *Sov. Phys. Dokl.* **12** (1967) 40.
6. YU. V. MALOV, *ibid.* **14** (1969) 545.
7. H. D. STROMBERG and D. R. STEPHENS, *Ceram. Bull.* **49** (1970) 1030.
8. N. SUZUKI, A. NAKAUE and O. OKUMA, *J. Jpn High Press. Inst.* **11** (1974) 301.
9. H. KATZMAN and W. F. LIBBY, *Science* **172** (1971) 1132.
10. Y. NOTSU, T. NAKAJIMA and N. KAWAI, *Mater. Res. Bull.* **12** (1977) 1079.
11. M. AKAISHI, H. KANDA, Y. SATO, N. SETAKA, T. OHSAWA and O. FUKUNAGA, *J. Mater. Sci.* **17** (1982) 193.
12. M. AKAISHI, Y. SATO, N. SETAKA, M. TSUTSUMI, T. OHSAWA and O. FUKUNAGA, *Ceram. Bull.* **62** (1983) 689.
13. F. P. BUNDY, H. T. HALL, H. M. STRONG and R. H. WENTORF Jr, *Nature* **176** (1955) 51.
14. P. S. DECARLI and J. C. JAMIESON, *Science* **133** (1961) 1821.
15. L. F. TRUEB, *J. Appl. Phys.* **39** (1968) 4707.
16. *Idem, ibid.* **42** (1971) 510.
17. T. AKASHI and A. B. SAWAOKA, *J. Am. Ceram. Soc.* **69** (1986) c-78.
18. *Idem, J. Mater. Sci.*, submitted.
19. T. AKASHI, V. LOTRICH, A. SAWAOKA and E. K. BEAUCHAMP, *J. Am. Ceram. Soc.* **68** (1985) c-322.
20. F. R. NORWOOD, R. A. GRAHAM and A. SAWAOKA, "Shock Waves in Condensed Matter", edited by Y. M. Gupta (Plenum, New York, 1986) p. 837.
21. T. AKASHI and A. B. SAWAOKA, *J. Mater. Sci.*, submitted.
22. H. P. KLUG and L. E. ALXANDER, "X-ray Diffraction Procedures" (Wiley, New York, 1975) p. 491.
23. V. I. TREFILOV, V. I. BORISENKO and O. N. GRIGOREV, *Sov. Phys. Dokl.* **19** (1975) 464.
24. R. C. DEVRIES, *Mater. Res. Bull.* **10** (1975) 1193.
25. K. KENDALL, *Nature* **272** (1978) 710.
26. L. M. STUPKINA, *Sov. Phys. Crystallogr.* **15** (1971) 728.
27. J. E. FIELD, "The Properties of Diamond" (Academic, New York, 1979) p. 282.
28. S. P. MARSH, "LASL Shock Hugoniot Data" (University of California, Berkeley, 1980) p. 28.
29. D. G. MORRIS, *Mater. Sci.* **15** (1981) 116.
30. D. RAYBOULD, *J. Mater. Sci.* **16** (1981) 589.
31. D. G. MORRIS, *Mater. Sci. Eng.* **57** (1983) 187.
32. L. DAVIDSON and R. A. GRAHAM, *Phys. Rep.* **55** (1979) 255.

Received 22 October 1986
and accepted 22 January 1987